

Arrival, Reversal, and Departure of Neurofilaments at the Tips of Growing Axons[□]

Atsuko Uchida and Anthony Brown*

Center for Molecular Neurobiology and Department of Neuroscience, The Ohio State University, Columbus, OH 43210

Submitted May 6, 2004; Revised June 8, 2004; Accepted June 16, 2004
Monitoring Editor: Paul Matsudaira

We have investigated the movement of green fluorescent protein-tagged neurofilaments at the distal ends of growing axons by using time-lapse fluorescence imaging. The filaments moved in a rapid, infrequent, and asynchronous manner in either an anterograde or retrograde direction (60% anterograde, 40% retrograde). Most of the anterograde filaments entered the growth cone and most of the retrograde filaments originated in the growth cone. In a small number of cases we were able to observe neurofilaments reverse direction, and all of these reversals occurred in or close to the growth cone. We conclude that neurofilament polymers are delivered rapidly and infrequently to the tips of growing axons and that some of these polymers reverse direction in the growth cone and move back into the axon. We propose that 1) growth cones are a preferential site of neurofilament reversal in distal axons, 2) most retrograde neurofilaments in distal axons originate by reversal of anterograde filaments in the growth cone, 3) those anterograde filaments that do not reverse direction are recruited to form the neurofilament cytoskeleton of the newly forming axon, and 4) the net delivery of neurofilament polymers to growth cones may be controlled by regulating the reversal frequency.

INTRODUCTION

Neurofilaments are space-filling cytoskeletal polymers that play a major role in the growth and maintenance of axonal caliber (Xu *et al.*, 1996). Studies on laboratory animals by using radioisotopic pulse labeling have demonstrated that neurofilaments are transported anterogradely along axons in slow component “a” of axonal transport at average rates of ~0.3–3 mm/d (0.003–0.03 $\mu\text{m/s}$; Lasek *et al.*, 1992). In contrast, studies on cultured neurons by using live-cell imaging of green fluorescent protein (GFP)-tagged neurofilament proteins have demonstrated that neurofilaments actually move at much faster rates and that the movements are also infrequent, bidirectional, and highly asynchronous (Roy *et al.*, 2000; Wang *et al.*, 2000; Wang and Brown, 2001). Based on these observations, we have proposed that neurofilaments are transported by fast motors and that the slow rate of movement is actually a temporal summation of rapid bidirectional movements interrupted by prolonged pauses (Brown, 2000, 2003a).

One intriguing feature of the live-cell imaging observations on neurofilaments is that these polymers move more rapidly than the rate of axon growth. For example, cultured neurons dissociated from the superior cervical ganglion of neonatal rats typically grow at rates of 4–30 $\mu\text{m/h}$ (0.001–0.008 $\mu\text{m/s}$; Argiro *et al.*, 1984; Kleitman and Johnson, 1989), depending on the substrate; yet, neurofilaments in these neurons move at average rates (excluding pauses) of 0.4–0.7 $\mu\text{m/s}$ (Roy *et al.*, 2000; Wang *et al.*, 2000; Wang and Brown,

2001). This suggests that anterogradely moving neurofilaments in the distal regions of growing axons may catch up with the advancing growth cone. Previous studies did not address this hypothesis because they were all performed in intermediate regions of the axon, far from the growth cone. Thus, in the present study, we investigated neurofilament transport at the tips of growing axons. We found that most anterograde neurofilaments in the distal axon catch up with and enter the growth cone. In addition, and to our surprise, some of these filaments subsequently reverse direction, exit the growth cone, and move back toward the cell body. Thus, local mechanisms at the axon tip can alter the direction of neurofilament movement, presumably by altering the activity of the neurofilament motors or their affinity for their cargo.

MATERIALS AND METHODS

Cell Culture

Neurons were dissociated from the superior cervical ganglia (SCG) of neonatal rats (P0–P2) and plated onto glass coverslips coated with poly-D-lysine (Sigma-Aldrich, St. Louis, MO; mol. wt. 70–150,000) and Matrigel (BD Biosciences, Bedford, MA). The cultures were maintained at 37°C in Liebovitz’s L-15 medium (phenol red free; Life Technologies, Grand Island, NY) supplemented with 0.6% glucose, 2 mM L-glutamine, 100 ng/ml 2.5S nerve growth factor (BD Biosciences), 10% adult rat serum (Harlan, Indianapolis, IN), and 0.5% hydroxypropylmethylcellulose (Methocel; Dow Corning, Midland, MI). For a more detailed description of the cell culture procedures, see Brown (2003b).

Transfection

The pEGFP-NFM expression vector, which directs the expression of the F64L/S65T variant of green fluorescent protein linked to the amino terminus of rat neurofilament protein M (GFP-NFM), has been described previously (Wang *et al.*, 2000). The plasmid was purified using an EndoFree Maxi plasmid purification kit (QIAGEN, Valencia, CA) and stored at a concentration of 1.2 mg/ml in TE (10 mM Tris/HCl, 1 mM EDTA, pH 8). For transfection, the DNA was diluted to 600 $\mu\text{g/ml}$ in 50 mM potassium glutamate, pH 7, and injected directly into the nucleus by using a FemtoJet pressure injector and an InjectMan NI2 motorized micromanipulator (Eppendorf,

Article published online ahead of print. Mol. Biol. Cell 10.1091/mbc.E04-05-0371. Article and publication date are available at www.molbiolcell.org/cgi/doi/10.1091/mbc.E04-05-0371.

[□] Online version of this article contains supporting material. Online version is available at www.molbiolcell.org.

* Corresponding author. E-mail address: brown.2302@osu.edu.

Westbury, NY) as described by Brown (2003b). The injection buffer also contained 1.25 mg/ml tetramethylrhodamine dextran (mol. wt. 10,000; Sigma-Aldrich) to permit visual confirmation of injection. Micropipettes were pulled from standard thick-wall borosilicate glass tubing (WPI, Sarasota, FL) by using a P-97 Flaming-Brown pipette puller (Sutter Instruments, Novato, CA). All injections were performed between 12 and 24 h after plating.

Live-Cell Imaging

Cells were observed in a sealed chamber containing culture medium 6–36 h after transfection. The temperature on the microscope stage was maintained at $\sim 35^{\circ}\text{C}$ with the use of a Nicholson ASI-400 airstream incubator (Nevtek, Burnsville, VA). To minimize photooxidative damage during imaging, the culture medium was mixed with EC-Oxyrase (1:100 dilution; Oxyrase, Mansfield, OH), 20 mM sodium succinate, and 20 mM sodium DL-lactate and incubated in an airtight syringe for 2 h at 37°C . Immediately before use, the medium was filtered through a $0.2\text{-}\mu\text{m}$ syringe filter to remove EC-Oxyrase particulates. Cells maintained in this medium retained active motile growth cones and apparently normal organelle movements for many hours, consistent with previous reports that the energy metabolism of cultured neurons is predominantly glycolytic (Bottenstein and Sato, 1979). Cells were observed by phase contrast and epifluorescence microscopy on a Nikon Quantum TE300 inverted microscope (Nikon, Garden City, NY) by using a Nikon $100\times/1.4$ numerical aperture Plan Apo phase contrast oil immersion objective and an FITC/EGFP filter set (HQ 41001; Chroma Technology, Brattleboro, VT). For a more detailed description of the live-cell imaging procedures, see Brown (2003b).

Image Processing and Analysis

Images were acquired using the Acquire and Acquire Time-Lapse functions in MetaMorph software (Universal Imaging, Downingtown, PA). Most imaging of living cells was performed using a Micromax 512BFT cooled charge-coupled device (CCD) camera (Roper Scientific, Trenton, NJ), and most imaging of fixed cells was performed using a CoolSNAP HQ cooled CCD camera (Roper Scientific). For time-lapse imaging, the epifluorescent illumination was attenuated fourfold or eightfold by using neutral density filters, and images were acquired with 1-s exposures at 4-s intervals. Motion analysis was performed by tracking the position of the leading ends of the filaments in successive time-lapse image frames by using the TrackPoints function in the Motion Analysis drop-in module of the MetaMorph software.

Immunostaining

For immunostaining, cultures were rinsed twice with warm phosphate-buffered saline (PBS) (37°C) and fixed using 4% (wt/vol) paraformaldehyde in PBS for 30 min. After fixation, the dishes were rinsed with PBS and then demembrated by treatment with 1% Triton X-100 in PBS for 15 min. Subsequently, the cultures were rinsed three times with PBS and then blocked with 4% normal goat serum (Jackson ImmunoResearch Laboratories, West Grove, PA) in PBS (blocking solution). The dishes were then incubated with primary antibody, rinsed, blocked again, and then incubated in fluorescently labeled secondary antibody. Finally, the dishes were rinsed with PBS and mounted using ProLong Antifade reagent (Molecular Probes, Eugene, OR). To visualize enhanced green fluorescent protein (EGFP)-NFM, we used a rabbit polyclonal primary antibody specific for GFP (Molecular Probes) and Alexa 488-conjugated goat anti-rabbit IgG secondary antibody (it was possible to detect the intrinsic EGFP fluorescence in fixed cells without immunostaining, but immunostaining provided a stronger signal). To visualize NFM, we used a phosphorylation-independent mouse monoclonal primary antibody (RMO255; gift of Dr. Virginia Lee, University of Pennsylvania, Philadelphia, PA; Lee *et al.*, 1987) and Alexa 568-conjugated goat anti-mouse IgG secondary antibody (Molecular Probes). All antibodies were used at a dilution of 1:200, and all antibody incubations were performed at 37°C for 45 min.

RESULTS

Experimental Strategy

The principal challenge to the observation of neurofilament movement in axons is that axonal neurofilaments are too close to each other to be resolved by fluorescence microscopy. In previous studies on cultured SCG neurons, we overcame this limitation by observing the movement of GFP-tagged fluorescent filaments through naturally occurring or photobleached gaps in the axonal neurofilament array in intermediate locations along the axon, far from the growth cone and cell body (Wang *et al.*, 2000; Wang and Brown, 2001). We were unable to use the natural gap method for the present study because neurofilaments tend to be more abundant in distal axons in these cultures, re-

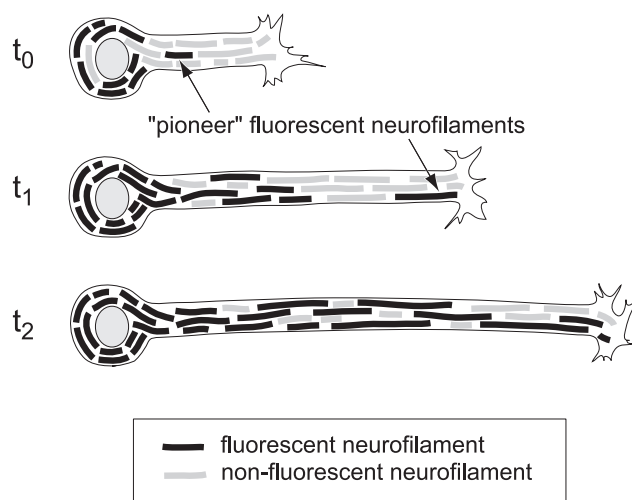


Figure 1. Experimental strategy. This diagram depicts the movement of GFP-tagged neurofilament protein out along the axon of a cultured neuron at early times after transfection. GFP-tagged neurofilaments form in the cell body (t_0) and subsequently move out into the axon in a time-dependent manner. To detect neurofilament movement in distal axons, we observed neurons at early times after transfection (t_1) when GFP-tagged neurofilaments first enter these regions. The movement of these “pioneer” fluorescent filaments can be detected at this time because the surrounding neurofilaments are not fluorescent. At later times after transfection (t_2), fluorescent filaments in the distal axon become more abundant and individual filaments cannot be resolved from their neighbors.

sulting in significantly fewer gaps close to growth cones. We were also reluctant to use the photobleaching method because we could not achieve sufficient bleaching of growth cones without causing the lamellipodial and filopodial extensions to retract, albeit temporarily. Thus, we developed an alternative approach that relies on the observation of neurons at early times after transfection, when GFP-tagged neurofilaments first enter the distal axons (Figure 1). To visualize neurofilaments, we transfected cultured SCG neurons with GFP-NFM fusion protein by nuclear injection of a plasmid DNA expression construct (see *Materials and Methods*). To determine the optimal time window for our observations, we investigated the time course of the appearance of neurofilaments containing GFP-NFM in distal axons (Figure 2). GFP-tagged neurofilaments first were present in the cell bodies several hours after transfection and subsequently extended out along the axons over the next 1–2 d, as reported previously (Ackerley *et al.*, 2000). By 6 h after transfection, GFP-tagged neurofilaments were present in most proximal axons but were largely absent from distal axons. By 12 h, short segments of GFP fluorescence, which may represent patches of incorporation along neurofilament polymers, were present in some distal axons. By 24 h, long GFP-tagged neurofilaments were evident in most distal axons. By 36 h after transfection, GFP-tagged neurofilaments were abundant along the entire length of all axons, forming a continuous overlapping array. These observations indicate that neurofilaments containing GFP-NFM first arrived in the distal axons of these neurons 12–24 h after transfection, so this is the time window that we chose for the present study.

Live-Cell Imaging of Distal Axons

We acquired time-lapse movies of the distal ends of 227 axons 12–24 h after transfection with GFP-NFM. The length

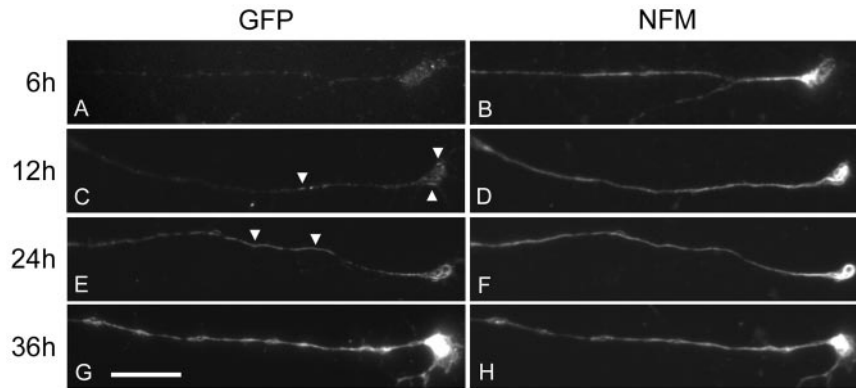


Figure 2. Time course of the appearance of GFP-NFM in distal axons. Cultured SCG neurons were fixed and processed for immunofluorescence microscopy 6–36 h after transfection with GFP-NFM fusion protein. Neurofilaments were visualized using RMO255 monoclonal antibody, which is specific for NFM, and GFP was visualized using a polyclonal antiserum (see *Materials and Methods*). Neurofilaments were present throughout the distal axons at all times (B, D, F, and H). (A) Six hours after transfection, GFP-tagged neurofilaments were largely absent from distal axons. (C) By 12 h, short segments of GFP fluorescence, which probably represented patchy incorporation along neurofilaments, were detectable in some distal axons (see arrowheads). (E) By 24 h, GFP-tagged neurofilaments were present in most distal axons (see arrowheads). (G) By 36 h, GFP-tagged neurofilaments were abundant throughout the distal regions of all axons. Bar, 10 μm .

of the distal axon that we could observe was dependent on its orientation in the field of view of the CCD camera ($67 \times 67 \mu\text{m}$), and ranged from 23 to 66 μm (average 47 μm). The duration of the time-lapse movies was limited by gradual photobleaching of the GFP fluorescence during observation; the average duration was 9.8 min. We analyzed the movement of all fluorescent structures in the time-lapse movies that exhibited a net displacement at least 3.3 μm (25 pixels). Using this criterion, we observed one moving structure every 7.2 min, which is similar to the frequency of movement that we reported in our previous studies on more proximal regions of these axons (Wang *et al.*, 2000; Wang and Brown, 2001). Moving structures were observed in 59% of the movies. The absence of moving structures in the other 41% of the movies was most probably due simply to the low frequency of movement and the short duration of our movies (on average, we observed only 1.3 moving structures per movie).

We classified the moving structures as filamentous if their length was greater than or equal to 1.3 μm (10 pixels) and punctate if their length was $<1.3 \mu\text{m}$. By this criterion, 299 (97%) of the moving structures were filamentous and 9 (3%) were punctate. The average length of the moving filaments was 6.1 μm (minimum 1.3 μm , maximum 24.4 μm ; $n = 299$). The diffraction-limited width and intensity of these filaments suggests that they represent single neurofilament polymers (Wang *et al.*, 2000), although we cannot exclude the possibility that they may represent bundles of two or more neurofilaments. It is not clear whether the punctate structures are short neurofilament polymers or patches of incorporation along neurofilament polymers or some other nonpolymeric form, but it is clear that they represent only a small proportion of the total moving protein. These observations are consistent with previous reports that neurofilament protein is transported in a predominantly filamentous form in these neurons (Roy *et al.*, 2000; Wang *et al.*, 2000; Wang and Brown, 2001).

The GFP-tagged filaments moved in a rapid, intermittent, and bidirectional manner that was very similar to the motile behavior observed in intermediate regions of these axons (Roy *et al.*, 2000; Wang *et al.*, 2000; Wang and Brown, 2001). Most filaments that paused resumed movement in the same

direction as they were moving before pausing. Many filaments exhibited transient reversals, often persisting for just one or two time intervals, but sustained reversals were relatively rare. Thus most moving filaments seemed to have a single preferred direction of movement, at least for the duration of our movies. The significance of the transient reversals is presently unclear. In theory, transient reversals could be generated by passive mechanisms such as elastic recoil of the filaments or the tracks along which they move or by the antagonistic actions of opposing motors. Because we are not confident that the transient reversals represent active motor-driven movement in both directions, we chose to consider only sustained reversals as true reversals in our analyses. For the purposes of the present study, we defined a sustained reversal as a change of direction that persisted for a distance of at least 10 μm or for a duration of at least 30 s. According to this criterion, 176 (59%) of the 299 filaments that we tracked moved anterogradely, 115 (38%) moved retrogradely, and 8 (3%) exhibited a sustained reversal (i.e., moved in both directions). We did not observe any filaments that exhibited more than one sustained reversal. The proportion of retrograde filaments was higher than in previous studies on intermediate axonal regions (17–31%; see Roy *et al.*, 2000; Wang *et al.*, 2000; Wang and Brown, 2001), indicating that a higher proportion of filaments move retrogradely in distal axons.

Arrivals, Departures, and Reversals

Figure 3 shows examples of two filaments that moved anterogradely. Most of the anterograde filaments originated outside of the field of view (i.e., from more proximal regions of the axon) and moved into the growth cone. Within the growth cone, these filaments often exhibited considerable movement, but they usually remained within the central region (C-domain) and rarely entered the peripheral lamellipodial and filopodial regions (P-domain). Longer filaments often looped back on themselves (Figure 3B). We presume that such movements give rise to the whorls of neurofilaments that are often observed in growth cones in these cultures (Figure 2F). Figure 4 shows an example of a filament that moved retrogradely. Most of the retrograde fila-

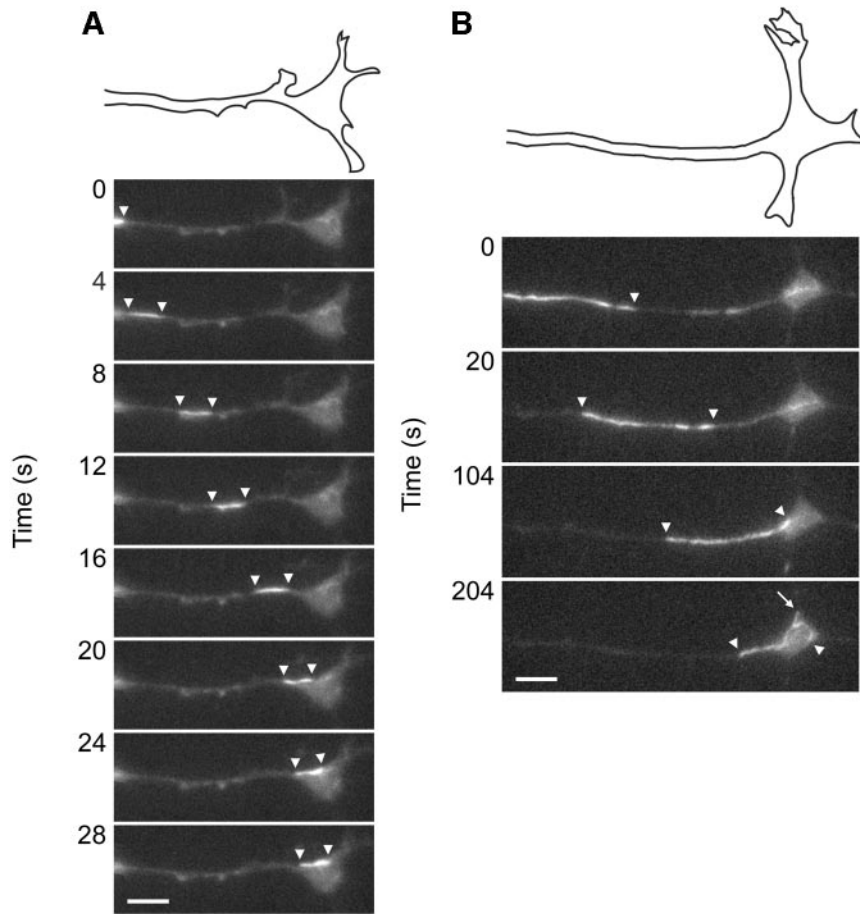


Figure 3. Movement of neurofilaments into the growth cone. The images shown here were selected from time-lapse movies in which images were acquired at 4-s intervals. The white arrowheads mark the leading and trailing ends of the filament. The drawing above each sequence of time-lapse images represents a manual trace of the outline of the distal axon and growth cone at the start of that sequence. (A) Arrival of a short fluorescent filament (3.2 μm in length) at the growth cone. The filament moved rapidly through the distal axon at an average velocity of 1.1 $\mu\text{m}/\text{s}$ and entered the growth cone, where it paused. (B) Arrival of a long fluorescent filament (16.7 μm in length) at the growth cone. The filament moved rapidly through the distal axon at an average velocity of 0.4 $\mu\text{m}/\text{s}$ and then entered the growth cone. After entering the growth cone, the leading portion of the filament circled back on itself and one section (see arrow) seemed to form a short hairpin loop. Subsequently, the trailing portion of the filament continued to move into the growth cone while the leading portion was stationary, causing the trailing portion to fold up on itself (see movie). This complex looping and folding behavior indicates that filaments can interact with motors at multiple sites along their length. The nonuniform intensity of the GFP fluorescence along this filament probably reflects nonuniform incorporation of GFP-NFM protein. The complete movies can be viewed online at www.molbiolcell.org. Proximal is left and distal is right. Bar, 5 μm .

ments originated in the growth cone and moved out of the field of view (i.e., toward more proximal regions of the axon). These filaments generally seemed somewhat fainter than the anterograde filaments because they originated from within the field of epifluorescent illumination and were therefore subjected to more photobleaching before their movement.

Figure 5 shows the trajectories of three anterograde filaments that entered the growth cone and three retrograde filaments that exited the growth cone. Some of the filaments moved continuously without pausing during the brief time that we were able to observe them (Figure 5, A, B, D, and F), whereas others exhibited movements interrupted by prolonged pauses (Figure 5, C and E). Of the 184 filaments that moved anterogradely (this includes the anterograde movements of the 8 filaments that reversed direction), 147 (80%) moved into the growth cone during the period of observation (Figure 6A). Of the 123 filaments that moved retrogradely (this includes the retrograde movements of the eight

filaments that reversed direction), 99 (81%) originated in the growth cone (Figure 6B). Overall, the frequency of arrivals in the growth cone was 4.0/h and the frequency of departures was 2.7/h.

Figure 7 shows examples of two filaments that reversed direction. Both filaments originated from outside of the field of view, entered the growth cone, paused, and then moved back into the axon and exited the field of view. Figure 8 shows the trajectories of three filaments that reversed direction in the growth cone and one that reversed direction before reaching the growth cone. In all cases, it can be seen that the filaments departed from the growth cone at a faster rate than they arrived (see below). In total, we observed eight sustained reversals. Five of these filaments reversed in the growth cone, and the others reversed at 13, 18, and 29 μm from the growth cone (Figure 9). The delay between arrival and departure at the growth cone (i.e., the residence time in the growth cone) ranged from 4 to 304 s (average 128 s; $n = 5$). Note, however, that the number of observed

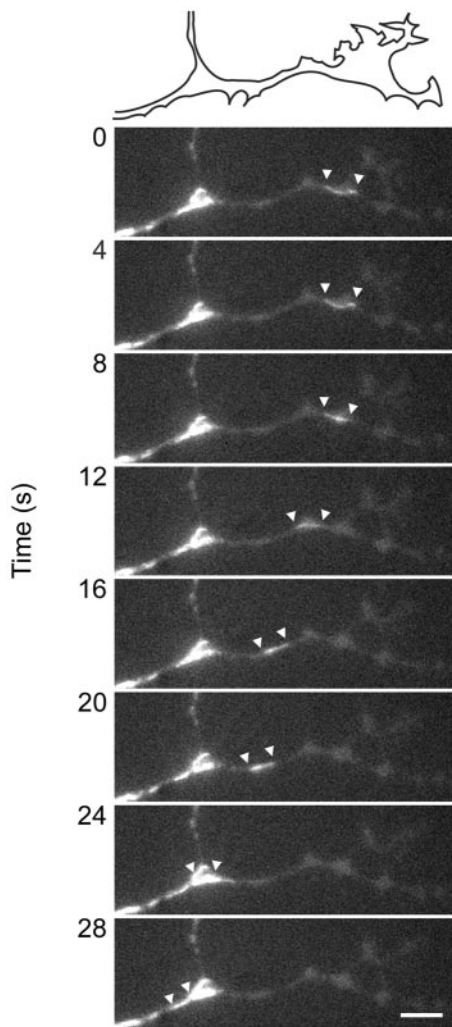


Figure 4. Departure of a neurofilament from the growth cone. Departure of a short fluorescent filament ($3.0\ \mu\text{m}$ in length) from the growth cone. The images shown here were selected from a time-lapse movie in which images were acquired at 4-s intervals. The white arrowheads mark the leading and trailing ends of the filament. The drawing above the time-lapse images represents a manual trace of the outline of the distal axon and growth cone at the start of this movie sequence. The filament moved rapidly through the distal axon at an average velocity of $0.8\ \mu\text{m/s}$. The complete movie can be viewed online at www.molbiolcell.org. The filament is not visible as it moves through the branch point in these still images, but it can be seen in the movie. Proximal is left and distal is right. Bar, $5\ \mu\text{m}$.

reversals and the average residence time are both likely to be underestimates because of the short duration of our movies (see *Discussion*). Seven of the filaments that reversed direction switched from anterograde to retrograde, and one switched from retrograde to anterograde (this reversal occurred $29\ \mu\text{m}$ from the growth cone). These data indicate that mechanisms in the axon tip can reverse the direction of neurofilament movement.

Velocities and Lengths

To analyze the pausing behavior of the filaments, we defined pausing as a movement of less than 1 pixel/s ($0.13\ \mu\text{m/s}$), which we estimate to be the precision limit of our

measurements (Wang *et al.*, 2000; Wang and Brown, 2001). For the 184 filaments that moved anterogradely (this includes the anterograde movements of the 8 filaments that reversed direction), the average time spent pausing was 65%. For the 123 filaments that moved retrogradely (this includes the retrograde movements of the 8 filaments that reversed direction), the average time spent pausing was 42%. The average velocity, excluding pauses and transient reversals, ranged from 0.13 to $1.13\ \mu\text{m/s}$ in the anterograde direction (average $0.39\ \mu\text{m/s}$; $n = 184$) and 0.24 – $1.24\ \mu\text{m/s}$ in the retrograde direction (average $0.56\ \mu\text{m/s}$; $n = 123$; Figure 10A). The peak velocity ranged from 0.20 to $2.26\ \mu\text{m/s}$ in the anterograde direction (average $0.85\ \mu\text{m/s}$; $n = 184$) and from 0.35 to $2.97\ \mu\text{m/s}$ in the retrograde direction (average $1.22\ \mu\text{m/s}$, $n = 123$; Figure 10B). The average and peak retrograde velocities were significantly faster than the corresponding anterograde velocities ($p < 0.001$; t test). Thus retrograde filaments moved more rapidly and paused less frequently than anterograde filaments. The average length of the moving filaments was $6.1\ \mu\text{m}$ (minimum $1.3\ \mu\text{m}$, maximum $24.4\ \mu\text{m}$; $n = 299$; Figure 10C). There was no apparent difference between the lengths of the anterograde and retrograde filaments ($p > 0.05$; Kolmogorov-Smirnov test).

DISCUSSION

Delivery of Neurofilaments to Growth Cones

Our previous studies on the axonal transport of neurofilaments in cultured neurons focused on intermediate portions of the axon, $>100\ \mu\text{m}$ from the cell body and growth cone (Wang *et al.*, 2000; Wang and Brown, 2001). In the present study, we turned our attention to the growth cone and distal end of the axon. We found that filaments moved rapidly into distal axons and that at least 80% of these filaments entered the growth cone. Thus, growth cones are the principal destination of anterogradely moving filaments in the distal axons of cultured neurons. Ninety seven percent of the moving structures that we observed were filamentous, which suggests that neurofilament proteins are delivered to the tips of growing axons primarily in the form of assembled polymers.

The movement of GFP-tagged neuronal intermediate filament proteins also has been studied in neuronal cell lines, although with somewhat different results. Shea and colleagues examined the movement of a GFP-tagged neurofilament protein in neurites of differentiated N2Ba/d1 neuroblastoma cells (Yabe *et al.*, 1999, 2001; Chan *et al.*, 2003), and Goldman and colleagues examined the movement of GFP-tagged peripherin in neurites of differentiated PC12 cells (Helfand *et al.*, 2003). At short times after neuritogenesis, neuronal intermediate filament proteins in both of these cell types existed predominantly in the form of punctate and short filamentous structures (Yabe *et al.*, 2001; Helfand *et al.*, 2003) that seemed to be enriched in growth cones (Chan *et al.*, 2003). Unlike the filamentous structures in our studies, these punctate structures reversed direction more frequently and paused less frequently. At later times, the neurofilament and peripherin proteins were predominantly filamentous, but punctate structures persisted in the growth cones (Yabe *et al.*, 2001; Helfand *et al.*, 2003).

Studies on vimentin in nonneuronal cells suggest that the precursors of intermediate filament assembly are punctate (Prahlad *et al.*, 1998), so it is possible that the punctate structures observed in N2Ba/d1 and PC12 cells may represent precursors of neurofilament assembly. Because the

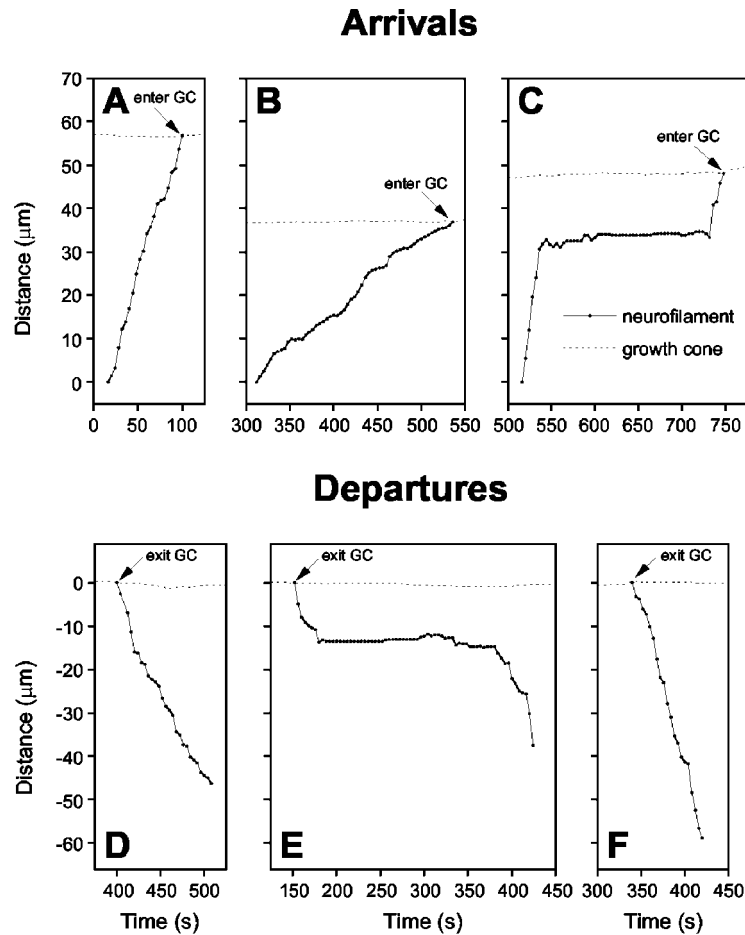


Figure 5. Motile behavior of anterograde and retrograde neurofilaments. Graphs of the movements of six representative filaments. The *y*-axis represents the distance of the filament along the axon from its initial location, and the *x*-axis represents the time elapsed since the start of the movie. Anterograde and retrograde movements are represented as positive and negative displacements, respectively. The solid lines represent the movement of the neurofilaments and the dotted lines represent the movement of the growth cones (tracked by measuring the location of the base of the growth cone). (A) A filament that moved rapidly and continuously in an anterograde direction at an average rate of $0.7 \mu\text{m/s}$ for 84 s. (B) A filament that moved rapidly and continuously in an anterograde direction at an average rate of $0.24 \mu\text{m/s}$ for 224 s. (C) A filament that moved rapidly in an anterograde direction at an average rate of $1.2 \mu\text{m/s}$ for 28 s, paused for 188 s, and then continued to move anterogradely at a rate of $0.7 \mu\text{m/s}$ for 16 s. (D) A filament that moved rapidly and continuously in a retrograde direction at an average rate of $0.5 \mu\text{m/s}$ for 108 s. (E) A filament that moved rapidly in a retrograde direction at an average rate of $0.5 \mu\text{m/s}$ for 28 s, paused for 200 s, and then continued to move retrogradely at an average rate of $0.7 \mu\text{m/s}$ for 44 s. (F) A filament that moved rapidly and continuously in a retrograde direction at an average rate of $0.7 \mu\text{m/s}$ for 80 s.

punctate structures move rapidly and seem to be enriched in growth cones, both the Shea and Goldman laboratories have suggested that these structures represent a rapid transport system capable of efficiently delivering unassembled neurofilament subunits to the distal regions of axons during axon growth (Chan *et al.*, 2003; Helfand *et al.*, 2003). In contrast, our data suggest that neurofilament proteins are delivered to growth cones primarily in the form of assembled polymers. The explanation for the difference is presently unclear, but it could be due to differences in neuronal intermediate filament dynamics in these different cell types or to differences in the expression level or assembly properties of the various GFP fusion proteins used in these studies.

Reversal of Neurofilaments in Growth Cones

In addition to the arrival of neurofilaments at the axon tip, we also observed numerous departures. Thirty-eight percent of the moving filaments in the distal axon moved retro-

gradely and 81% of these filaments originated in the growth cone. There are two possible explanations for the origin of these retrograde filaments: either they assembled *de novo* in the growth cones or they originated by reversal of anterograde filaments. Although we cannot exclude the possibility of *de novo* assembly based on our present data, we have not observed any indication of lengthening or shortening of filaments in the growth cone that might be indicative of filament assembly and disassembly. In addition, the length distributions of the anterograde and retrograde filaments were not significantly different from each other, and our observations indicate that at least some of the retrograde filaments clearly did originate by reversal of anterograde filaments. For these reasons, we think it is most likely that the retrograde neurofilaments originated by reversal of anterograde filaments.

In total, we observed 147 filaments enter growth cones and 99 exit, yet we observed only five reversals in the

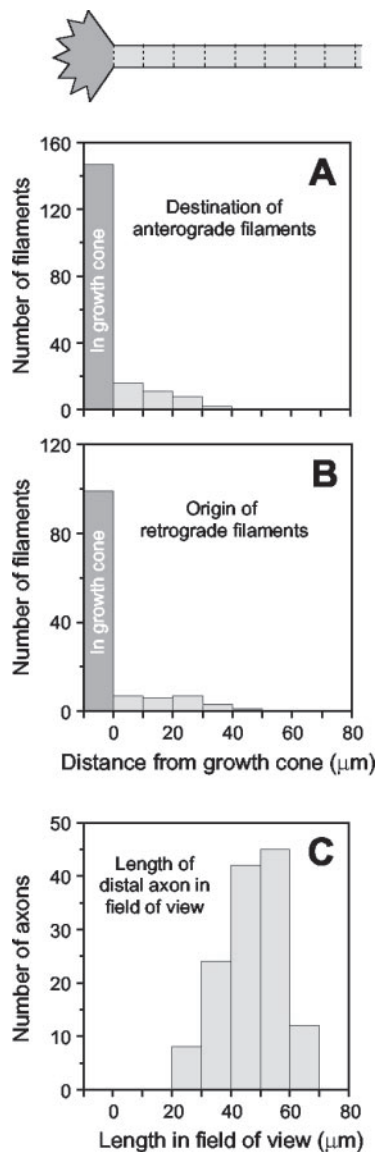


Figure 6. Origins and destinations. (A) Destinations of the anterogradely moving filaments that we tracked ($n = 184$). (B) Origins of the retrogradely moving filaments that we tracked ($n = 123$). 80% of the anterograde filaments moved into the growth cone and 81% of the retrograde filaments originated in the growth cone. (C) Lengths of the distal axons observed, which was dictated by the orientation of the distal axon relative to the field of view of the CCD camera. Note that it is possible that some or all of the anterograde filaments that did not reach the growth cone during the period of time that we observed them may have done so eventually if it had been possible to observe the axons for longer periods. Similarly, some or all of the retrograde filaments that did not originate in the growth cone during our movies may have done so originally if it had been possible to observe the axons for longer periods. Thus, it is possible that an even higher proportion of the filaments entered and exited the growth cone than is apparent in this figure.

growth cone. At first glance, these data seem to indicate that only a small fraction of the retrograde filaments could have originated by reversal. However, it is important to note that our movies were relatively short (average 9.8 min) and that we could only confirm the occurrence of a reversal if we observed the same filament arrive and depart within one

movie. Because there is no reason to believe that the delay between the arrival and departure of a reversing filament should necessarily be shorter than the duration of our movies, it seems likely that the number of retrograde filaments that originated by reversal is greater than the number of reversals that we actually observed. To test this hypothesis, it will be necessary to observe growth cones for longer durations, but we are currently limited to short movie durations due to photobleaching of the GFP fluorescence during image acquisition.

The observation of reversals in the present study on distal regions of these axons contrasts with our previous studies on intermediate regions of these axons in which we did not observe any reversals (Wang *et al.*, 2000; Wang and Brown, 2001). One possible explanation for this discrepancy is that neurofilaments only reverse direction at the axon tip, but it is premature to draw such a conclusion because the number of filaments that we tracked in the previous studies (69 and 72 filaments) was much lower than in the present study (299 filaments). Moreover, reversals were observed in intermediate axonal regions in the study of Roy *et al.* (2000) for five out of a total of 73 filaments, although it should be noted that those filaments apparently exhibited unusually erratic behavior, reversing multiple times within the short period of time that they were tracked. Although it remains to be proven, it seems most likely to us that sustained reversals can occur throughout these axons and that the low frequency of observed reversals reflects the fact that the filaments typically pause for longer durations than the duration of our movies before reversing direction (see above). Nevertheless, the fact that all the reversals that we observed in the present study occurred in or close to the growth cone does suggest that growth cones may be a preferential site of reversals, at least in distal axons.

What Is the Mechanism of Reversal?

Our velocity measurements indicate that the neurofilaments moved faster and paused less often in the retrograde direction than in the anterograde direction, which suggests that anterograde and retrograde movements are generated by distinct motors. This difference was not apparent in previous studies, perhaps because the number of filaments tracked was too few to achieve statistical significance (Roy *et al.*, 2000; Wang and Brown, 2001; Wang *et al.*, 2000). The identity of the neurofilament motors and the tracks along which they move is not known, but several lines of evidence point to the role of microtubules and microtubule motors. Neurofilaments copurify with dynein and components of the dynactin complex, and antibodies and pharmacological inhibitors of dynein partially inhibit the movement of neurofilaments along microtubules *in vitro* (Shah *et al.*, 2000). In transgenic mice, overexpression of the p50/dynamitin subunit of dynactin results in neurofilamentous accumulations in peripheral nerves (LaMonte *et al.*, 2002). In PC12 cells, overexpression of p50/dynamitin results in a redistribution of peripherin to the distal regions of the neurites and a depletion in proximal neurites and in the cell body, whereas microinjection of H1 antibody, which recognizes KIF5A and KIF5C (Cai *et al.*, 2001), leads to an accumulation of peripherin in the cell body and a depletion from neurites (Helfand *et al.*, 2003). Finally, conditional knockout of KIF5A in postnatal mice by using a Cre-lox strategy results in the accumulation of neurofilaments in the cell bodies of DRG neurons and a depletion from the peripheral axons (Xia *et al.*, 2003).

These data suggest that neurofilaments are cargoes for microtubule motor proteins and that their reversal involves

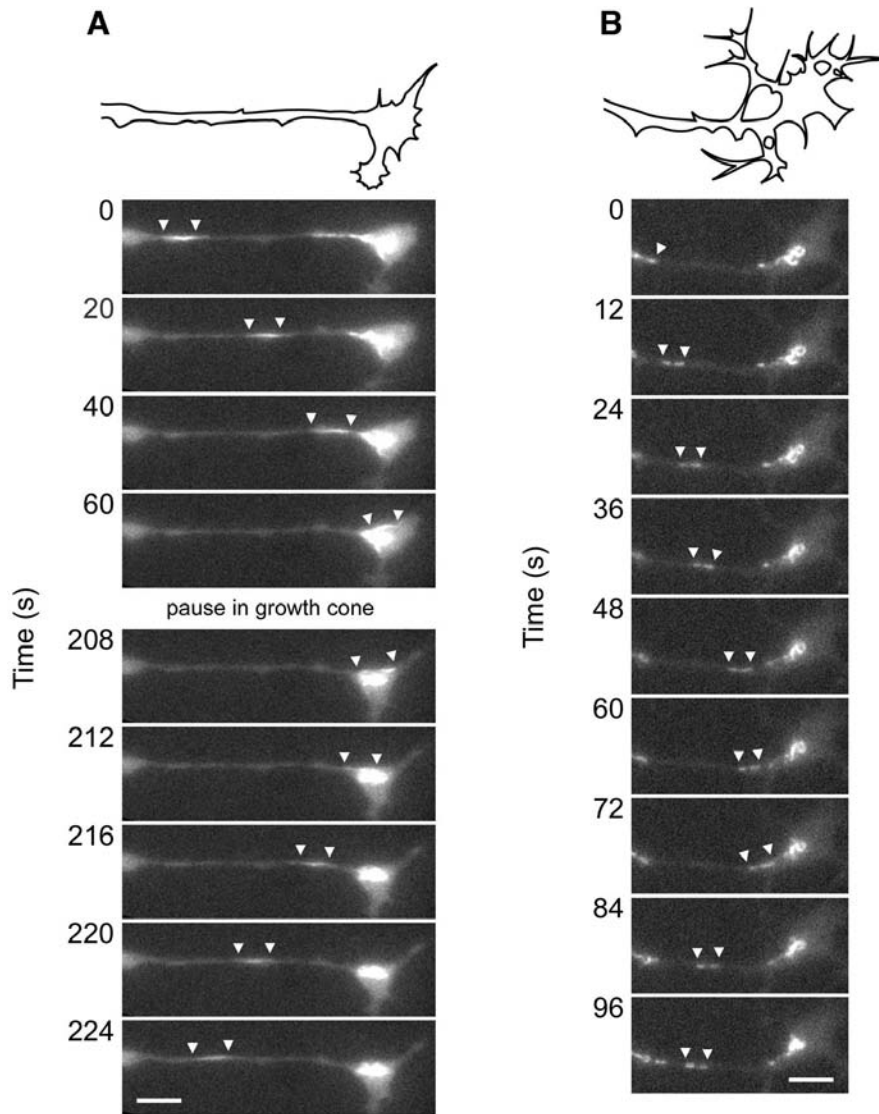


Figure 7. Reversal of neurofilaments in the growth cone. The images shown here were selected from time-lapse movies in which images were acquired at 4-s intervals. The white arrowheads mark the leading and trailing ends of the filament. The drawing above each sequence of time-lapse images represents a manual trace of the outline of the distal axon and growth cone at the start of that sequence. (A) A short filament that moved into growth cone at an average velocity of $0.93 \mu\text{m/s}$, paused for 164 s, and then reversed direction and moved back into the axon at an average velocity of $0.34 \mu\text{m/s}$. (B) A short filament that moved anterogradely at an average velocity of $0.29 \mu\text{m/s}$, paused at the base of the growth cone for 4 s, and then reversed direction and moved back into the axon at an average velocity of $0.29 \mu\text{m/s}$. Note that this filament occurs as two short fluorescent segments separated by a nonfluorescent region. We assume that these two segments are two portions of the same filament because they moved in complete synchrony; the nonuniformity of the fluorescence presumably reflects nonuniform incorporation of GFP-NFM. The complete movies can be viewed online at www.molbiolcell.org. Proximal is left and distal is right. Bar, $5 \mu\text{m}$.

a switch between kinesin-dependent anterograde movement and dynein-dependent retrograde movement. The mechanism of directional switching of bidirectional cargoes is an issue of considerable interest in the field of intracellular motility. One possible mechanism is that both plus-end and minus-end directed motors are simultaneously bound and active and the direction of movement results from a sort of molecular “tug-of-war” (Carson *et al.*, 2001). Another possible model is that both motors are bound but their activity is coordinated so that only motors of one directionality are active at one time (Gross, 2003). At present, there is insufficient data on neurofilament transport to distinguish between these models.

What Is the Function of Retrograde Neurofilament Transport?

The existence of a retrograde component to slow axonal transport was proposed originally by Griffin and colleagues based on their analysis of the redistribution of neurofilaments and other cytoskeletal proteins in isolated segments of peripheral nerves from *Ola* mice, which exhibit slow Wallerian degeneration (Glass and Griffin, 1991, 1994; Watson *et al.*, 1993). The observation of retrograde neurofilament movement in cultured nerve cells by ourselves and others has provided direct support for their conclusions, but the function of this movement remains unclear. Why do

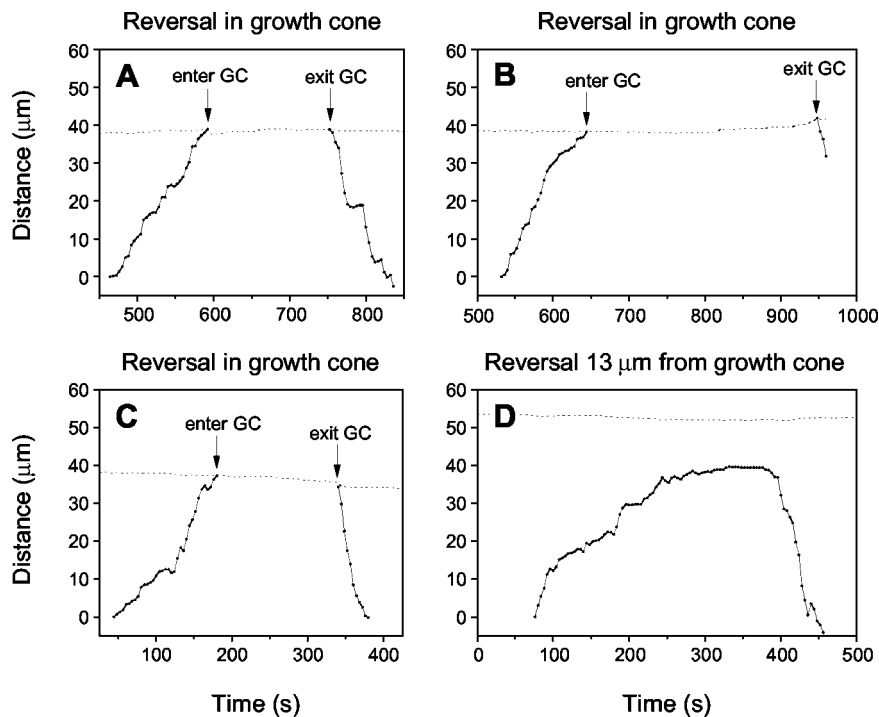


Figure 8. Motile behavior of reversing neurofilaments. Graphs of the movement of four filaments that exhibited sustained reversals. (A–C) Traces for three filaments that reversed in the growth cone. (D) Trace for one filament that reversed 13 μm proximal to the growth cone. The solid lines represent the movement of the neurofilaments and the dotted lines represent the movement of the growth cones (tracked by measuring the location of the base of the growth cone). Note that the growth cones do not advance or retract more than a few micrometers during the several minutes of time represented in these graphs.

neurons invest metabolic energy to move axonal neurofilaments retrogradely in axons? One possibility is that bidirectional movement may allow for more versatility in the regulation of neurofilament distribution along axons than would be possible if neurofilaments could only move anterogradely. For example, neurons may actively regulate the distribution of axonal neurofilaments along the length of axons by locally modulating the balance of anterograde and retrograde movements and pauses. Because neurofilaments are the principal determinants of axonal morphology in large myelinated axons, we expect that the balance of anterograde and retrograde movements would have a profound influence on axonal morphology. Dynamic regulation of this balance could contribute to the dramatic remodeling of the neurofilament cytoskeleton that occurs during development and regeneration. It is possible that bidirectional movement may also provide an elegant mechanism for regulating the net delivery of neurofilaments to the axon tip during axon growth. For example, local regulation of the reversal of neurofilaments at the axon tip could provide a mechanism to rapidly adjust the net delivery of neurofilaments to the growth cone to match the short-term needs of the growing axon.

A Hypothesis for the Fate of Neurofilaments at the Axon Tip

To explain our data on the arrival, reversal, and departure of neurofilaments at the axon tip, we propose the following working hypothesis (see the Flash animation movie online at www.molbiolcell.org). We consider that neurofilaments are delivered to the tips of growing axons in a rapid and intermittent manner. Reversals occur throughout the axon, but they are more frequent at the axon tip. The neuron matches

the net delivery of neurofilaments to the needs of the growing axon by controlling their retention in the growth cone. Specifically, we propose that the neuron exports neurofilaments from the cell body at a constant rate in these growing axons, and controls the rate of recruitment into the growing axon by modulating the frequency of reversals in the growth cone. This allows for tight regulation of neurofilament number at the axon tip in response to events at the growth cone. For example, when axons are growing slowly on a relatively nonpermissive substrate, the frequency of arrivals at the axon tip may exceed the demands of the elongating axon (see first phase of animation). In this situation, we propose that mechanisms in the axon tip reverse the direction of neurofilaments, allowing them to exit the growth cone in a retrograde direction. This prevents neurofilament accumulation at the growth cone. It is possible that neurofilaments pause for some time in the growth cone before reversing direction (see above), but for convenience the residence time in the growth cone in the animation is depicted as being relatively short. The retrogradely moving neurofilaments that depart from the growth cone move back into more proximal regions of the axon. If axons encounter a more growth-promoting substrate (see second phase of animation), they will advance more rapidly. Now, the rate of delivery of neurofilaments more closely matches the demands of the elongating axon. To meet this demand, the reversal of neurofilaments in the growth cone is down-regulated and more neurofilaments that arrive in the growth cone are recruited into the nascent axonal neurofilament array.

When axons reach their targets, they cease to elongate and enter a phase of radial growth (for simplicity, we ignore the

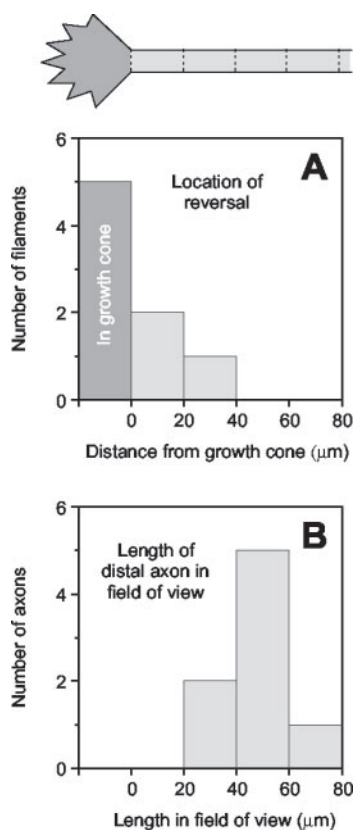


Figure 9. The growth cone is a preferential site of reversals. (A) Location of reversals for the eight filaments that were observed to reverse direction. (B) Lengths of the distal axons observed in those eight movies, which was dependent on the orientation of the distal axon relative to the field of view of the CCD camera. Note that all of the reversals occurred in or close to the growth cone.

possibility of interstitial growth; see Bray, 1984). It is well established that most of this radial growth is due to the accumulation of neurofilaments in the axons (Williamson *et al.*, 1996; Sanchez *et al.*, 2000). In this model, we consider that when axons stop growing all arriving neurofilaments reverse direction and move back into the axon where they pause and become incorporated into the expanding axonal neurofilament cytoskeleton. Thus we propose that both anterogradely and retrogradely moving filaments contribute to the accumulation of neurofilaments in axons during radial growth. As the axon matures, the distribution of neurofilaments along the axon is actively remodeled by the actions of motors of opposing directionality. After axons have reached their mature caliber, neurofilaments that reach the axon tip may be degraded by calcium dependent proteases (Roots, 1983; Paggi and Lasek, 1987; Garner, 1988; not shown in the animation). Although this model is speculative, it does explain our present data in a way that is consistent with what we know about neurofilaments in axons, and it does make several testable predictions. For example, one clear prediction is that the reversal of neurofilaments is regulated and that neurofilaments reverse more frequently at the tips of slower growing axons and less frequently at the tips of faster growing axons. In future, we plan to test this prediction.

ACKNOWLEDGMENTS

We thank Kitty Jensen and Yanping Yan in the Brown laboratory for help throughout this project. This study was funded by a grant to A.B. from the

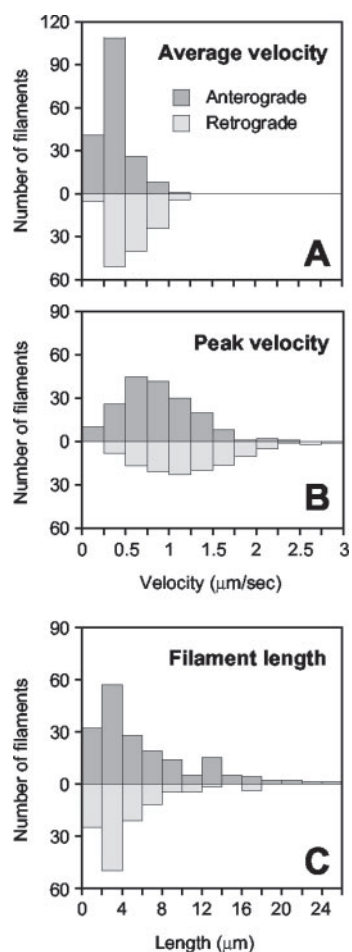


Figure 10. Velocities and lengths of moving neurofilaments. (A) Average velocity and (B) peak velocity for 184 filaments that moved anterogradely and 123 filaments that moved retrogradely. The average velocity excludes pauses, which we defined as movements of less than one pixel per second ($0.131 \mu\text{m/s}$). We estimate this to be the precision limit of our measurements (see *Materials and Methods*). Peak velocity is defined as the maximum velocity attained in a single time-lapse interval. The average and peak velocities were significantly faster in the retrograde direction than in the anterograde direction ($p < 0.001$; t test). (C) Lengths of 299 filaments that moved. The lengths ranged from 1.3 to $24.4 \mu\text{m}$ (average $6.1 \mu\text{m}$). There was no apparent difference between the lengths of the anterograde and retrograde filaments ($p > 0.05$; Kolmogorov-Smirnov test).

National Institutes of Health. A.U. was supported for part of this work by a Research Fellowship for Young Scientists from the Japanese Society for the Promotion of Science.

REFERENCES

- Ackerley, S., Grierson, A.J., Brownlees, J., Thornhill, P., Anderton, B.H., Leigh, P.N., Shaw, C.E., and Miller, C.C. (2000). Glutamate slows axonal transport of neurofilaments in transfected neurons. *J. Cell Biol.* 150, 165–176.
- Argiro, V., Bunge, M.B., and Johnson, M.I. (1984). Correlation between growth form and movement and their dependence on neuronal age. *J. Neurosci.* 4, 3051–3062.
- Bottenstein, J.E., and Sato, G.H. (1979). Growth of a rat neuroblastoma cell line in serum-free supplemented media. *Proc. Natl. Acad. Sci. USA* 76, 514–517.
- Bray, D. (1984). Axonal growth in response to experimentally applied mechanical tension. *Dev. Biol.* 102, 379–389.

- Brown, A. (2000). Slow axonal transport: stop and go traffic in the axon. *Nat. Rev. Mol. Cell. Biol.* *1*, 153–156.
- Brown, A. (2003a). Axonal transport of membranous and nonmembranous cargoes: a unified perspective. *J. Cell Biol.* *160*, 817–821.
- Brown, A. (2003b). Live-cell imaging of slow axonal transport in cultured neurons. *Methods Cell Biol.* *71*, 305–323.
- Cai, Y., Singh, B.B., Aslanukov, A., Zhao, H., and Ferreira, P.A. (2001). The docking of kinesins, KIF5B and KIF5C, to Ran-binding protein 2 (RanBP2) is mediated via a novel RanBP2 domain. *J. Biol. Chem.* *276*, 41594–41602.
- Carson, J.H., Cui, H., and Barbarese, E. (2001). The balance of power in RNA trafficking. *Curr. Opin. Neurobiol.* *11*, 558–563.
- Chan, W.K., Yabe, J.T., Pimenta, A.F., Ortiz, D., and Shea, T.B. (2003). Growth cones contain a dynamic population of neurofilament subunits. *Cell Motil. Cytoskeleton* *54*, 195–207.
- Garner, J.A. (1988). Differential turnover of tubulin and neurofilament proteins in central nervous system neuron terminals. *Brain Res.* *458*, 309–318.
- Glass, J.D., and Griffin, J.W. (1991). Neurofilament redistribution in transected nerves: evidence for bidirectional transport of neurofilaments. *J. Neurosci.* *11*, 3146–3154.
- Glass, J.D., and Griffin, J.W. (1994). Retrograde transport of radiolabeled cytoskeletal proteins in transected nerves. *J. Neurosci.* *14*, 3915–3921.
- Gross, S.P. (2003). Dynactin: coordinating motors with opposite inclinations. *Curr. Biol.* *13*, R320–322.
- Helfand, B.T., Loomis, P., Yoon, M., and Goldman, R.D. (2003). Rapid transport of neural intermediate filament protein. *J. Cell Sci.* *116*, 2345–2359.
- Kleitman, N., and Johnson, M.I. (1989). Rapid growth cone translocation on laminin is supported by lamellipodial not filopodial structures. *Cell Motil. Cytoskeleton* *13*, 288–300.
- LaMonte, B.H., Wallace, K.E., Holloway, B.A., Shelly, S.S., Ascano, J., Tokito, M., Van Winkle, T., Howland, D.S., and Holzbaur, E.L. (2002). Disruption of dynein/dynactin inhibits axonal transport in motor neurons causing late-onset progressive degeneration. *Neuron* *34*, 715–727.
- Lasek, R.J., Paggi, P., and Katz, M.J. (1992). Slow axonal transport mechanisms move neurofilaments relentlessly in mouse optic axons. *J. Cell Biol.* *117*, 607–616.
- Lee, V.M., Carden, M.J., Schlaepfer, W.W., and Trojanowski, J.Q. (1987). Monoclonal antibodies distinguish several differentially phosphorylated states of the two largest rat neurofilament subunits (NF-H and NF-M) and demonstrate their existence in the normal nervous system of adult rats. *J. Neurosci.* *7*, 3474–3488.
- Paggi, P., and Lasek, R.J. (1987). Axonal transport of cytoskeletal proteins in oculomotor axons and their residence times in the axon terminals. *J. Neurosci.* *7*, 2397–2411.
- Prahlad, V., Yoon, M., Moir, R.D., Vale, R.D., and Goldman, R.D. (1998). Rapid movements of vimentin on microtubule tracks: kinesin-dependent assembly of intermediate filament networks. *J. Cell Biol.* *143*, 159–170.
- Roots, B.I. (1983). Neurofilament accumulation induced in synapses by leupeptin. *Science* *221*, 971–972.
- Roy, S., Coffee, P., Smith, G., Liem, R.K.H., Brady, S.T., and Black, M.M. (2000). Neurofilaments are transported rapidly but intermittently in axons: implications for slow axonal transport. *J. Neurosci.* *20*, 6849–6861.
- Sanchez, I., Hassinger, L., Sihag, R.K., Cleveland, D.W., Mohan, P., and Nixon, R.A. (2000). Local control of neurofilament accumulation during radial growth of myelinating axons in vivo: selective role of site-specific phosphorylation. *J. Cell Biol.* *151*, 1013–1024.
- Shah, J.V., Flanagan, L.A., Janmey, P.A., and Leterrier, J.-F. (2000). Bidirectional translocation of neurofilaments along microtubules mediated in part by dynein/dynactin. *Mol. Biol. Cell* *11*, 3495–3508.
- Wang, L., and Brown, A. (2001). Rapid intermittent movement of axonal neurofilaments observed by fluorescence photobleaching. *Mol. Biol. Cell* *12*, 3257–3267.
- Wang, L., Ho, C.-L., Sun, D., Liem, R.K.H., and Brown, A. (2000). Rapid movement of axonal neurofilaments interrupted by prolonged pauses. *Nat. Cell Biol.* *2*, 137–141.
- Watson, D.F., Glass, J.D., and Griffin, J.W. (1993). Redistribution of cytoskeletal proteins in mammalian axons disconnected from their cell bodies. *J. Neurosci.* *13*, 4354–4360.
- Williamson, T.L., Marszalek, J.R., Vechio, J.D., Bruijn, L.I., Lee, M.K., Xu, Z., Brown, R.H., Jr., and Cleveland, D.W. (1996). Neurofilaments, radial growth of axons, and mechanisms of motor neuron disease. *Cold Spring Harbor Symp. Quant. Biol.* *61*, 709–723.
- Xia, C.H., Roberts, E.A., Her, L.S., Liu, X., Williams, D.S., Cleveland, D.W., and Goldstein, L.S. (2003). Abnormal neurofilament transport caused by targeted disruption of neuronal kinesin heavy chain KIF5A. *J. Cell Biol.* *161*, 55–66.
- Xu, Z.S., Marszalek, J.R., Lee, M.K., Wong, P.C., Folmer, J., Crawford, T.O., Hsieh, S.T., Griffin, J.W., and Cleveland, D.W. (1996). Subunit composition of neurofilaments specifies axonal diameter. *J. Cell Biol.* *133*, 1061–1069.
- Yabe, J.T., Chan, W.K.-H., Chylinski, T.M., Lee, S., Pimenta, A., and Shea, T.B. (2001). The predominant form in which neurofilament subunits undergo axonal transport varies during axonal initiation, elongation and maturation. *Cell Motil. Cytoskeleton* *48*, 61–83.
- Yabe, J.T., Pimenta, A., and Shea, T.B. (1999). Kinesin-mediated transport of neurofilament protein oligomers in growing axons. *J. Cell Sci.* *112*, 3799–3814.